Nanoreactors

A Supramolecular Tubular Nanoreactor

Zhi-Qiang Li, Ying-Ming Zhang, Yong Chen, and Yu Liu*[a]

Abstract: The extremely strong noncovalent complexation between the rigid host of phthalocyanine-bridged β-cyclodextrins and the amphiphilic guest carboxylated porphyrin is employed to construct a hollow tubular structure as a supramolecular nanoreactor. A representative coupling reaction occurs in the hydrophobic interlayers of the tubular walls in pure water at room temperature, leading to an enhancement of ten times higher reaction rate without any adverse effect on catalytic activity and conversion.

In the last two decades, nanometer-scaled hollow structures have attracted growing interest owing to their fascinating properties in material conversion and delivery,[1] and construction protocols for various self-assembled hollow nanostructures with cage-like, cavity-like, vesicle-like, tube-like, and porous topology have been successfully established.[2] Among them, tubular nanostructures possess several considerable advantages compared with nanostructures with other topologies.[3] Firstly, the tubular structures may have reduced weight, better mechanic stability, and larger surface-to-volume area. Secondly, the open-ended feature of tubular arrays enables not only the simultaneous interactions of cylindrical internal and external surfaces with substrates, but also the delivery of exogenous products, which jointly maximize the catalytic performance.[4] These advantages are also used by natural systems such as in the coating protein of the tobacco mosaic virus, cytoplasmic microtubules, and endoplasmic reticulum.[5] Typically, the enveloping membrane of chloroplast in some plants can form vesicle or tubular structures, and the biosynthesis of lipids takes place under the catalysis of enzymes attached to the surface of these hollow structures.[6] However, the potential of artificial tubular nanostructures as reactors has barely been uncovered, despite the fact that these tubular nanostructures, which have tunable diameters ranging from the micro- down to nano-scale, can provide spatially confined reaction chambers and channels for materials synthesis and substance exchange. Herein, we report a hollow tubular nanostructure constructed through reasonably strong host–guest associations[7]
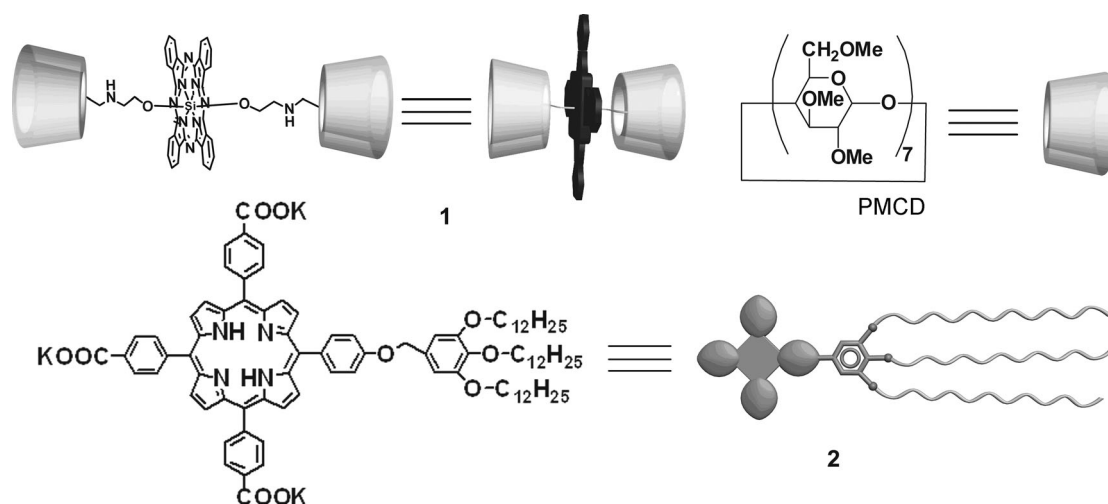
[a] Z.-Q. Li, Dr. Y.-M. Zhang, Prof. Dr. Y. Chen, Prof. Dr. Y. Liu
Department of Chemistry, State Key Laboratory of
Elemento-Organic Chemistry, Nankai University
Collaborative Innovation Center of Chemical Science and Engineering
Tianjin 300071 (P.R. China)
E-mail: yuliu@nankai.edu.cn

Supporting information for this article is available on the WWW under
http://dx.doi.org/10.1002/chem.201402612.

between permethylated β-cyclodextrin (PMCD) dimers with rigid silicon(IV) phthalocyanine cores (**1**) and carboxylated porphyrin bearing long hydrophobic tails (**2**), followed by the supramolecular assembly of **1/2** couples (Scheme 1). In this nanostructure, the rigid-core-tethered host (**1**) of silicon(IV) phthalocyanine axially bridged with two permethylated β-cyclodextrins (PMCD) can adjust the curvature of organic nanotubes to avoid any undesirable formation of micelles or vesicles,[8] whereas carboxylated porphyrin **2** not only provides the anchoring sites for catalytic centers, but also offer a hydrophobic microenvironment to readily accommodate the active binding domains. As a result, the tubular nanostructure can promote highly efficient catalytic reactions under environmentally benign conditions.

The dimeric host, **1**, possessing a silicon(IV) phthalocyanine core, was prepared according to the reported method,[9] and the amphiphilic guest, **2**, with hydrophobic tail was synthesized by the reaction of phenolic hydroxyl-substituted porphyrin with a benzyl bromide derivative bearing alkyl chains under basic conditions (Figures S1–S3, see the Supporting Information). Subsequently, UV/Vis spectroscopic experiments were performed to quantitatively investigate the host–guest binding behaviors in aqueous solution. As shown in Figure 1, the incorporation of **1** with **2** underwent a clear complexation-induced bathochromic shift from 680 to 689 nm, accompanied by a clear isosbestic point at 685 nm. Similarly, the absorbance changes of **1** became steady in the presence of 1 equivalent of **2**, indicating 1:1 host–guest binding stoichiometry between **1** and **2** (Figure 1, inset).[10] In addition, the complex stability constant (K_s) was calculated to be $1.3\times10^7\,\mathrm{M}^{-1}$ by analyzing the sequential changes in absorbance intensity (ΔA) of **1** at varying concentrations of **2** by using a nonlinear least-squares curve-fitting method.[11] Moreover, the peak at m/z 1619.4413 in the mass spectrum was assigned to $[\mathbf{1}+\mathbf{2}-3\mathrm{K}^+]^{3-}$ (Figure S4, see the Supporting Information). These results jointly reveal that the porphyrin backbone of **2** was concurrently associated with two PMCD cavities of **1** to form a highly stable inclusion complex in water, and more importantly, this extremely strong binding would facilitate the eventual formation of supramolecular tubules as described below (Scheme 2).

Direct morphological information of the tubular nanostructure based on the host–guest complexation of **1** with **2** was provided by scanning electron microscopy (SEM) and transmission electron microscopy (TEM). As can be discerned from Figure 2A, SEM images of an air-dried equimolar solution of **1** and **2** exclusively display cylindrical tubules with an open-ended hollow space. Moreover, TEM images gave detailed structural information, in which the aggregates constructed from complex **1·2** clearly show hollow tubular structures with

These are not the final page numbers! ↗↗

Scheme 1. Structural illustration of compounds **1**, **2**, and permethyl β-cyclodextrin (PMCD).
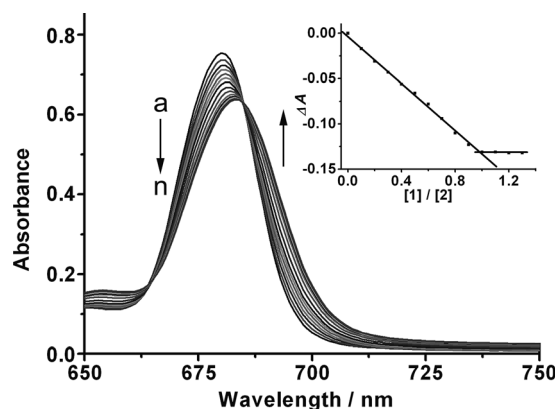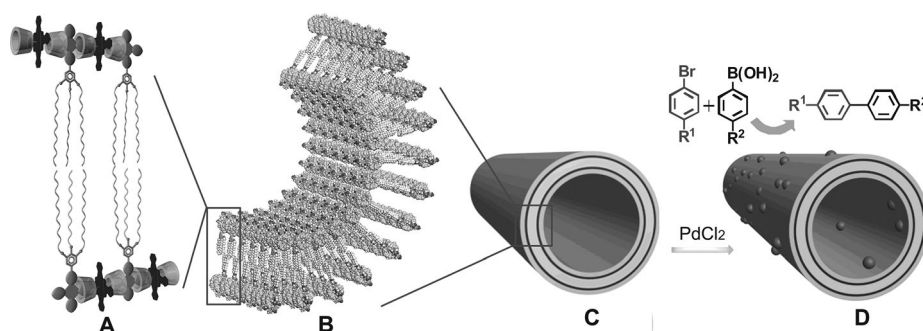

Figure 1. UV/Vis spectral changes of Q band of **2** (5.0×10^{-6} M) upon addition of 0–1.3 equivalents of **1** (from a to n) in pH 7.2 phosphate buffer solution at 25 °C. Inset: the absorption changes versus **1**/**2** molar ratio recorded at $\lambda = 680$ nm.

of guest molecule **2** was 4.1 nm, the wall thickness of the nanotubes essentially corresponds to a bilayer array of complex **1·2** along the vertical section of the tubular wall (Figure S5, see the Supporting Information). In addition, the powder X-ray diffraction (XRD) spectrum of the nanotubes exhibited a diffraction peak with a *d* spacing of 3.6 nm ($2\theta = 2.46°$), which could be assigned to the size of complex **1·2** along the axial direction of the nanotubes (Figure S6, see the Supporting Information). Therefore, by combining this information, we can reasonably infer the structure of the nanotubes is as follow: the interior and exterior surfaces of the nanotubes are composed of the highly stable PMCD/porphyrin-associated units with rigid phthalocyanine spacers, whereas the hydrophobic alkyl chains interlace with each other in the middle of the tubular walls (Scheme 2).

The self-assembly in solution was investigated by ¹H NMR, DOSY, and dynamic light scattering (DLS) experiments. In ¹H NMR spectroscopy, the aromatic protons of free **2** showed dramatic broadening of the peaks, but the proton signals became sharp and clear in the presence of **1** (Figure S7, see the Supporting Information). These large disparities in the NMR peak patterns suggest that the formation of the inclusion complex **2·**PMCD can greatly deter the negatively charged porphyrins from π-aggregation in water.[12] Compared with the diffusion coefficient of the individual compounds **1** (1.87×10^{-10} m² s⁻¹) and **2** (4.03×10^{-10} m² s⁻¹) from DOSY experiments, the complex **1·2** gave a relatively low diffusion coefficient (1.52×10^{-10} m² s⁻¹) at the same concentration (1.0×10^{-3} M), indicating that the complex **1·2** can diffuse as one entity with a slower diffusion rate and a higher molecular weight (Fig-

Scheme 2. Schematic representation of the tubular self-assembly. A) Building blocks of **1** and **2** in the formation of the nanotube wall. B) Self-assembly of the nanotube wall. C) Supramolecular nanotube with a bilayer array of **1·2** complex. D) Test reaction catalyzed by Pd@NT.

uniform size (Figure 2B and 2C). On the basis of the TEM analysis, the average inner and outer diameters of the obtained nanotubes were around 182 and 200 nm, respectively, with a wall thickness of 9 nm. Considering that the stretched length

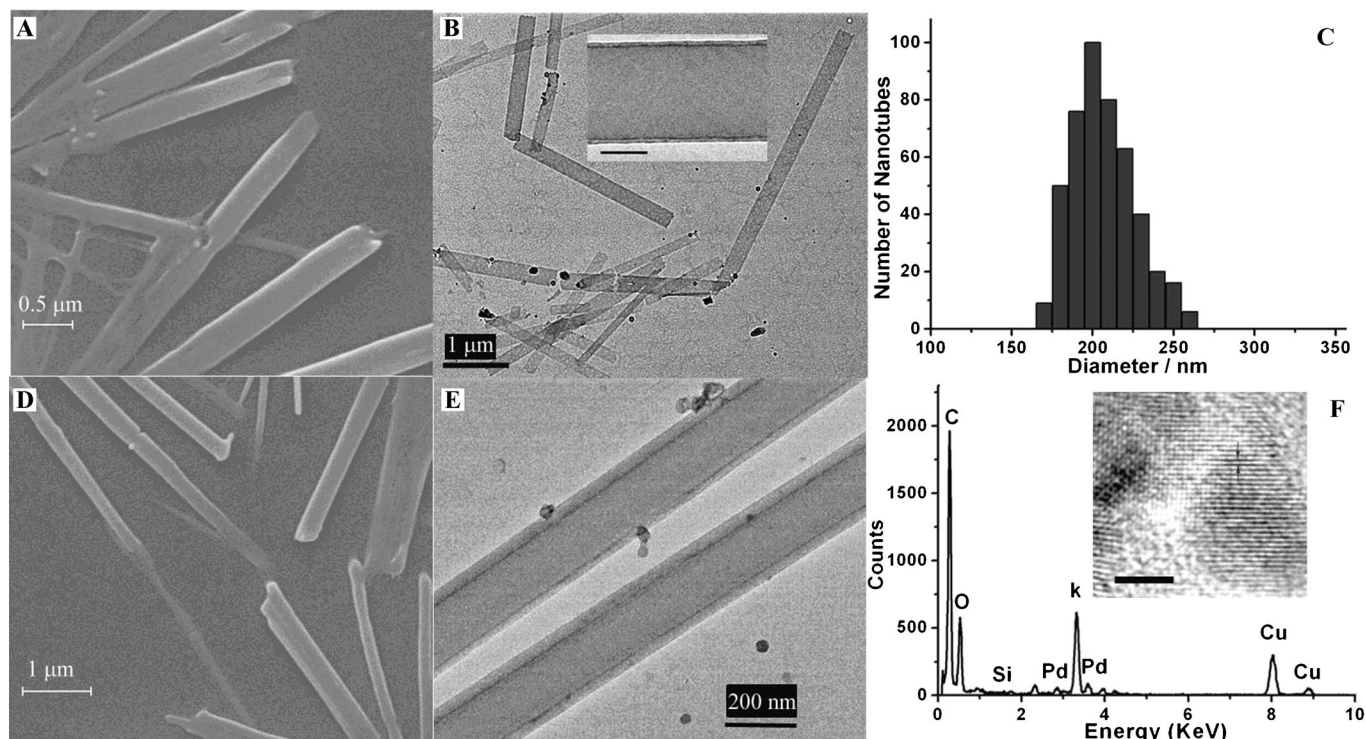**↖↖ These are not the final page numbers!**

Figure 2. Morphological characterization of the tubular assembly. A) Typical SEM and B) typical TEM images of the tubular assembly (inset: magnified image of tubules with 100 nm scale bar). C) Diameter size distribution of the tubular assembly obtained from TEM image statistics. D) Typical SEM and E) typical TEM images of Pd@NT. F) The corresponding EDX spectrum of Pd@NT (inset: magnified image of Pd@NT wall with 2 nm scale bar).

ure S8, see the Supporting Information) than the individual components.[13] In addition, the DLS results for complex **1·2** also display an average hydrodynamic radius of 1.2 μm, corresponding to the existence of large-scaled aggregates in aqueous solution (Figure S9, see the Supporting Information). Moreover, microscopy experiments were also performed to obtain morphological information about the supramolecular assembly in solution and the solid state. The cryo-TEM image (Figure S10a, see the Supporting Information) shows the mutual spatial arrangement of assembly **1·2** as tubular structures with an average diameter of around 200 nm, which is consistent with the corresponding value measured from Figure 2. Additionally, the SEM images of freeze-dried samples (Figure S10b) also exhibited typical tubular structures with a similar size. In contrast, as shown in Figure S11a in the Supporting Information, only amorphous morphological structures could be observed in **1**. It is also confirmed that the amphiphilic compound **2** can self-assemble to a closed vesicular structure with a diameter of around 200 nm, which is much smaller than the supramolecular nanotube **1·2** (Figures S12 and S13, see the Supporting Information). These results jointly demonstrate the formation of tubular assemblies of **1·2**.

From the structural features of the tubular nanostructures, one can see that there were numerous pendant carboxylic acid groups located at the periphery of the porphyrins, groups that could act as anchoring sites for various metal-based catalysts. Moreover, the zeta potential of the tubular self-assembly was measured as −34.5 mV and this negatively charged surface would facilitate the binding of metal catalysts (Figure S14,

see the Supporting Information). For example, palladium chloride ($PdCl_2$) in aqueous solution could be conveniently introduced onto the interior and exterior surfaces of the nanotube to form Pd^{2+}-loaded nanotubes (Pd@NT) through the electrostatic interaction between the carboxylic acid groups and metal catalysts. Tubular nanostructures similar to those in Figure 2A and B were observed in the SEM and TEM images of Pd@NT, suggesting that the nanotube remained in its original structure after attaching Pd^{2+} (Figure 2D and 2E). In addition, energy-dispersive X-ray (EDX) analysis demonstrated the existence of Pd^{2+} on the tubular surfaces (Figure 2F), giving the characteristic peaks of Pd^{2+} attached on the interior and exterior surfaces. Further TEM analysis provided direct information about the structure of the Pd@NT wall. The selected area electron diffraction (SAED) pattern gave the polycrystalline structure of the Pd@NT wall (Figure S15, see the Supporting Information), and the high-resolution TEM image of the edge of the Pd@NT wall presented lattice fringes of 0.22 nm, which coincided with the lattice structures of Pd^{2+} (Figure 2F, inset). Consequently, it is reasonable to deduce that the surfaces of the hollow microstructures have been successfully loaded with Pd^{2+} catalyst. In addition, from inductively coupled plasma (ICP) analysis, the content of the Pd^{2+} ions was measured as 2.62 mg L^{-1} in a 3×10^{-5} mol L^{-1} solution of Pd@NT; that is, one Pd^{2+} ion was carried by 1.23 complexes of **1·2** on average.

After the ability of the nanotubes to be loaded with metal catalysts was validated, Suzuki–Miyaura coupling reactions, which consist of ligand exchange followed by a reductive coupling reaction between aryl halides and phenylboronic acid de-

These are not the final page numbers! ↗↗

rivatives,[14] were selected to explore the catalytic capability of the metal-loaded nanotubes, Pd@NT. Some representative catalytic results for reactions preformed at ambient temperature and pressure in water without the need of any organic cosolvent are listed in Table 1. As shown in Table 1, the catalytic activity of Pd@NT is applicable to various substrates, ultimately leading to the excellent isolated yields (93–99%) in only one

Table 1. Suzuki–Miyaura coupling reaction catalyzed by Pd@NT.

$$Br{-}\bigcirc{-}R^1 + (HO)_2B{-}\bigcirc{-}R^2 \xrightarrow[K_2CO_3,\ r.t.,\ in\ water]{Pd@NT} R^1{-}\bigcirc{-}\bigcirc{-}R^2$$

| Entry | R^1 | R^2 | Yields of isolated product [%] | | |
			cycle 1	cycle 2	cycle 3
1	H	H	96	95	96
2	OCH_3	H	94	94	94
3	CH_3	H	97	97	96
4	CN	H	99	99	98
5	NO_2	H	98	98	97
6	$COCH_3$	H	96	96	95
7	H	OCH_3	97	95	96
8	OCH_3	OCH_3	93	94	93
9	CH_3	OCH_3	95	95	95
10	CN	OCH_3	99	97	96
11	NO_2	OCH_3	98	99	97
12	$COCH_3$	OCH_3	94	95	93

hour, which was a comparably higher efficiency than results under the same experimental conditions.[15] Moreover, the Pd@NT catalyst can be easily recovered and reused for many catalytic cycles without any loss of reactivity and conversion ratio.

Taking the coupling reaction of 4-nitrobromobenzene with phenylboronic acid as an example, some control experiments were carried out to prove the prominent enhancement in the Pd@NT-catalyzed coupling reactions. It was found that Pd@NT can greatly accelerate the chemical reaction rates, and 95% conversion was readily obtained in 30 min (Figure 3, a). In comparison, the use of pristine $PdCl_2$, containing the same Pd^{2+} content, instead of Pd@NT resulted in a dramatically decreased
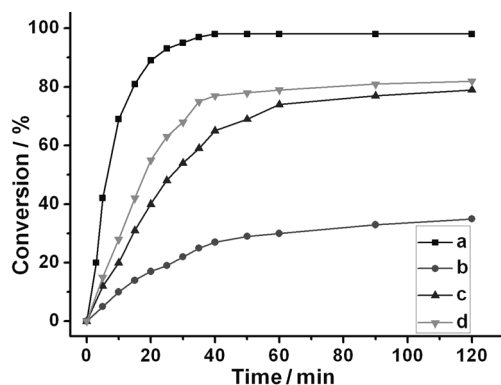

Figure 3. Suzuki–Miyaura reaction of 4-nitrobromobenzene with phenylboronic acid catalyzed by: a) Pd@NT in pure water, b) $PdCl_2$ in pure water, c) $PdCl_2$ in 1:1 THF/water mixed solvent, and d) Pd-loaded vesicle **2**.

reaction rate, and only 35% conversion to the cross-coupling product was achieved even after extending the reaction time to two hours (Figure 3, b). A control experiment using pristine $PdCl_2$ in the presence of potassium benzoate was carried out to mimic any effect from the carboxylic acid groups on Pd@NT. No obvious change in yield was observed with potassium benzoate and a similar yield to the previous pristine $PdCl_2$ experiment (33%) was observed. In addition, a moderate yield of isolated product of up to 80% was obtained by using a THF/water mixed solvent system to increase the solubility of the starting reactants (Figure 3, c). Presumably, the lack of efficient supporting materials blocks the sufficiently close contact of reactant molecules to catalysts, which limits any further increases in the yield.[16] Moreover, the individual compound **2** was found to self-assemble to closed vesicular structures (Figures S12 and S13), which showed a significantly lower conversion ratio than Pd@NT (Figure 3, d). In particular, within the initial 15 min, the conversion ratio of Pd-loaded vesicle **2** was less than 50% of the corresponding value of Pd@NT under the same conditions. A possible reason may be that the catalytic reaction only occurred at the exterior surface of the fully sealed vesicles, leading to the decreased catalytic activity compared with Pd@NT, where both interior and exterior surfaces of the nanotubes actively participate in the catalytic reaction (Figure S13). Moreover, no catalytic activity was observed by using the individual component **1** as it lacked the loaded Pd^{2+}. These results confirm that the spatial arrangement of supramolecular tubules plays a crucial role in the promotion of the coupling reaction. Furthermore, a plot of ln[4-nitrobromobenzene] versus reaction time was essentially linear (Figure S16, see the Supporting Information), thus attesting to a pseudo-first-order reaction.[17] The slope of the straight line provided the value of the observed rate constant (k_{obs}). The k_{obs} value of the Pd@NT-catalyzed coupling reaction was calculated as $1.63 \times 10^{-3}\ s^{-1}$, which was 10 times higher than the corresponding control groups.

The binding geometry involving the tubular nanoreactor was further confirmed by ^{1}H NMR spectra. By comparison with the spectra of complex **1·2**, a broadened peak in the range from 6.8 to 7.5 ppm was assigned to the characteristic signals of biphenyl derivative of 4-biphenylcarbonitrile in D_2O (Figure S17, see the Supporting Information). As shown in the rotating-frame Overhauser effect spectroscopy (ROESY) experiment, a clear nuclear Overhauser enhancement (NOE) cross-correlation between the protons of 4-biphenylcarbonitrile and alkyl chains was observed (peaks A, Figure S18, see the Supporting Information). In addition, the coupling reaction was also performed with a wide range of Pd^{2+} concentrations (the mole ratio of Pd^{2+} to substrate was fixed at 3%). It is shown that a relatively high yield could be obtained even when the concentration of complex **1·2** in Pd@NT was as low as $2 \times 10^{-5}\ M$ (Table S1, see the Supporting Information). In this case, through a calculation of the binding constant of **1** and **2** ($1.3 \times 10^7\ M^{-1}$), as well as the concentrations of host and guest, more than 94% of complex **1·2** still exists in solution. Furthermore, to investigate the advantage of the nanotube in the coupling reaction, 2 equivalents of PMCD as the competitive host was

↖↖ **These are not the final page numbers!**

added to the solution of tubule **1·2**. As shown in the TEM image, the tubular structure was seriously destroyed in the presence of PMCD (Figure S11b). Clearly, the complex **1·2** is disassembled to complex **2·PMCD**; the K_S value for PMCD and negatively charged porphyrins is up to $10^8 \, \mathrm{M}^{-1}$.[18] Under such circumstances, only 53% yield was obtained with an excess amount of PMCD. These results demonstrate that the biphenyl derivative of 4-biphenylcarbonitrile was located in the hydrophobic domains of alkyl chain interlayers in tubules **1·2**, which can draw the reactant and catalyst molecules closer together and thereby promotes the catalytic reaction.

In conclusion, we constructed supramolecular nanotubes through noncovalent molecular assembly of bridged PMCD dimers and amphiphilic guests in water. Structurally, the preorganized and rigid host–guest complex ensures the homogeneous dispersion of active binding sites. The introduction of carboxylic acid groups immobilizes the metal catalysts on the surfaces of the tubules. Functionally, the resulting Pd@NT display enhanced catalytic activity for the Suzuki–Miyaura cross-coupling reaction, even for those substrates with low water solubility, with the added benefits of using environmentally friendly reaction media and conditions. This work also highlights that supramolecular tubules can not only act as supporting materials, but also promote the positive conversion from reactants to products. In addition, we believe that the judicious use of functionalized cyclodextrins and metallized substrates will continue to energize and expand the exciting uses of supramolecular tubular nanoarchitectures into other fields of asymmetric synthesis and chiral materials.

Experimental Section

Preparation of tubular assembly Pd@NT

The freeze-dried 1:1 inclusion complex of **1** and **2** (99 mg, 0.02 mmol) were added into distilled water (10 mL), then PdCl$_2$ (18 mg, 0.1 mmol) was added. The mixture was stirred for 12 h at room temperature in the dark. The suspension was centrifuged at 8000 rpm for 10 min to remove the undissolved PdCl$_2$. Subsequently, the Pd-loaded organic nanotube (Pd@NT) was purified by dialysis (molecular weight cutoff 3500) in distilled water several times until the water outside the dialysis tube contained a negligible amount of Pd^{2+}.

Acknowledgements

[1] a) Y. Xia, P. Yang, Y. Sun, Y. Wu, B. Mayers, E. Gates, Y. Yin, F. Kim, H. Yan, *Adv. Mater.* **2003**, *15*, 353–389; b) K. J. C. van Bommel, A. Friggeri, S. Shinkai, *Angew. Chem.* **2003**, *115*, 1010–1030; *Angew. Chem. Int. Ed.* **2003**, *42*, 980–999; c) T. F. A. De Greef, M. M. J. Smulders, M. Wolffs, A. P. H. J. Schenning, R. P. Sijbesma, E. W. Meijer, *Chem. Rev.* **2009**, *109*, 5687–5754; d) T. Aida, E. W. Meijer, S. I. Stupp, *Science* **2012**, *335*, 813–817; e) D. T. Bong, T. D. Clark, J. R. Granja, M. R. Ghadiri, *Angew. Chem.* **2001**, *113*, 1016–1041; *Angew. Chem. Int. Ed.* **2001**, *40*, 988–1011.

[2] a) M. Yoshizawa, M. Tamura, M. Fujita, *Science* **2006**, *312*, 251–254; b) Q. Li, W. Zhang, O. S. Miljanic, C.-H. Sue, Y.-L. Zhao, L. Liu, C. B. Knobler, J. F. Stoddart, O. M. Yaghi, *Science* **2009**, *325*, 855–859; c) Y. Yamamoto, T. Fukushima, Y. Suna, N. Ishii, A. Saeki, S. Seki, S. Tagawa, M. Taniguchi, T. Kawai, T. Aida, *Science* **2006**, *314*, 1761–1764; d) L. C. Palmer, C. J. Newcomb, S. R. Kaltz, E. D. Spoerke, S. I. Stupp, *Chem. Rev.* **2008**, *108*, 4754–4783; e) C. Park, I. H. Lee, S. Lee, Y. Song, M. Rhue, C. Kim, *Proc. Natl. Acad. Sci. USA* **2006**, *103*, 1199–1203; f) G. Chen, M. Jiang, *Chem. Soc. Rev.* **2011**, *40*, 2254–2266; g) H. Jin, W. Huang, X. Zhu, Y. Zhou, D. Yan, *Chem. Soc. Rev.* **2012**, *41*, 5986–5997; h) R. Chakrabarty, P. S. Mukherjee, P. J. Stang, *Chem. Rev.* **2011**, *111*, 6810–6918.

[3] a) Y. Yamamoto, G. Zhang, W. Jin, T. Fukushima, N. Ishii, A. Saeki, S. Seki, S. Tagawa, T. Minari, K. Tsukagoshi, T. Aida, *Proc. Natl. Acad. Sci. USA* **2009**, *106*, 21051–21056; b) A. J. Dirks, R. J. M. Nolte, J. J. L. M. Cornelissen, *Adv. Mater.* **2008**, *20*, 3953–3957; c) M. Reches, E. Gazit, *Science* **2003**, *300*, 625–627; d) L. Zhi, T. Gorelik, J. Wu, U. Kolb, K. Müllen, *J. Am. Chem. Soc.* **2005**, *127*, 12792–12793.

[4] a) Y. Tang, L. P. Zhou, J. X. Li, Q. Luo, X. Huang, P. Wu, Y. G. Wang, J. Y. Xu, J. C. Shen, J. Q. Liu, *Angew. Chem.* **2010**, *122*, 4012–4016; *Angew. Chem. Int. Ed.* **2010**, *49*, 3920–3924; b) C. Park, M. S. Im, S. Lee, J. Lim, C. Kim, *Angew. Chem.* **2008**, *120*, 10070–10074; *Angew. Chem. Int. Ed.* **2008**, *47*, 9922–9926; c) J. H. Kim, M. Lee, J. S. Lee, C. B. Park, *Angew. Chem.* **2012**, *124*, 532–535; *Angew. Chem. Int. Ed.* **2012**, *51*, 517–520; d) X. Zhao, F. Pan, H. Xu, M. Yaseen, H. Shan, C. A. E. Hauser, S. Zhang, J. R. Lu, *Chem. Soc. Rev.* **2010**, *39*, 3480–3498.

[5] Z. Huang, S.-K. Kang, M. Banno, T. Yamaguchi, D. Lee, C. Seok, E. Yashima, M. Lee, *Science* **2012**, *337*, 1521–1526.

[6] R. H. Köhler, P. Schwille, W. W. Webb, M. R. Hanson, *J. Cell Sci.* **2000**, *113*, 3921–3930.

[7] J.-M. Lehn, *Supramolecular Chemistry: Concepts and Perspectives*, Wiley-VCH, Weinheim, **1995**.

[8] T. Shimizu, M. Masuda, H. Minamikawa, *Chem. Rev.* **2005**, *105*, 1401–1443.

[9] J. T. F. Lau, P.-C. Lo, W.-P. Fong, D. K. P. Ng, *Chem. Eur. J.* **2011**, *17*, 7569–7577.

[10] K. Kano, R. Nishiyabu, T. Asada, Y. Kuroda, *J. Am. Chem. Soc.* **2002**, *124*, 9937–9944.

[11] Y. Inoue, K. Yamamoto, T. Wada, S. Everitt, X.-M. Gao, Z.-J. Hou, L.-H. Tong, S.-K. Jiang, H.-M. Wu, *J. Chem. Soc. Perkin Trans. 2* **1998**, 1807–1816.

[12] Z.-Q. Li, Y.-M. Zhang, H.-Z. Chen, J. Zhao, Y. Liu, *J. Org. Chem.* **2013**, *78*, 5110–5114.

[13] Y. Liu, Z. Wang, X. Zhang, *Chem. Soc. Rev.* **2012**, *41*, 5922–5932.

[14] N. Miyaura, A. Suzuki, *Chem. Rev.* **1995**, *95*, 2457–2483.

[15] M. Mondal, U. Bora, *Green Chem.* **2012**, *14*, 1873–1876.

[16] L. Shao, B. Zhang, W, Zhang, S. Y. Hong, R. Schlögl, D. S. Su, *Angew. Chem.* **2013**, *125*, 2168–2171; *Angew. Chem. Int. Ed.* **2013**, *52*, 2114–2117.

[17] B. P. Carrow, J. F. Hartwig, *J. Am. Chem. Soc.* **2011**, *133*, 2116–2119.

[18] a) Z.-Y. Gu, D.-S. Guo, M. Sun, Y. Liu, *J. Org. Chem.* **2010**, *75*, 3600–3607; b) Z.-Q. Li, Y.-M. Zhang, D.-S. Guo, H.-Z. Chen, Y. Liu, *Chem. Eur. J.* **2013**, *19*, 96–100.

COMMUNICATION

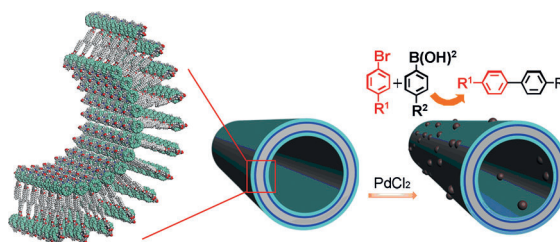Z.-Q. Li, Y.-M. Zhang, Y. Chen, Y. Liu*

■■ – ■■

A Supramolecular Tubular Nanoreactor

Reaction in a nanotube: A tubular nanoarchitecture is constructed by the noncovalent complexation of phthalocyanine-bridged bis(β-cyclodextrin)s and amphiphilic porphyrin. The nanotube is utilized as a supramolecular nanoreactor to drive a Pd-catalyzed coupling reaction within its hydrophobic interlayers under environmentally friendly conditions.

◤◤ These are not the final page numbers!